Supporting Information

CoO_x nanoparticles loaded on carbon spheres with synergistic effects for effective inhibition of shuttle effect in Li-S batteries

Ning Chai [a,b,1], Yujie Qi [b,c,1], Junnan Chen [b,c], Qinhua Gu [b,c], Ming Lu [b,d], Xia Zhang [a*], Bingsen Zhang [b,c*]

a Department of Chemistry, College of Science, Northeastern University, Shenyang 110819, China

b Shenyang National Laboratory for Materials Science, Institute of Metal Research, Chinese Academy of Sciences, Shenyang 110016, China

c School of Materials Science and Engineering, University of Science and Technology of China, Shenyang 110016, China

d The Joint Laboratory of MXene Materials, Key Laboratory of Functional Materials Physics and Chemistry of the Ministry of Education, Key Laboratory of Preparation and Application of Environmental Friendly Materials of the Ministry of Education, Jilin Normal University, Changchun 130103, China

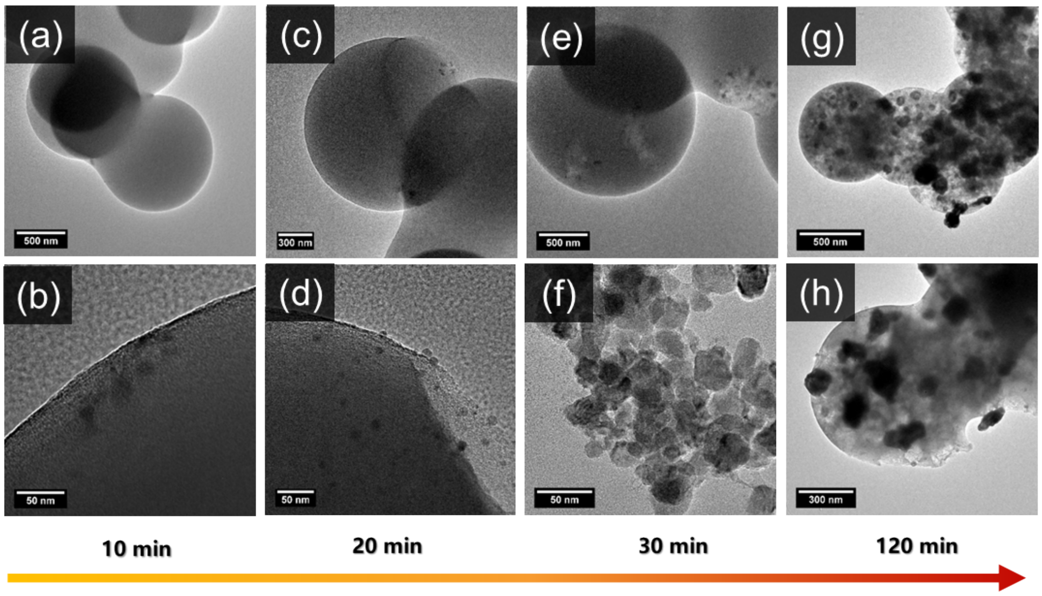

Fig. S1. TEM images of CoO_x/CS composites heated at 600 °C for 10 min (a, b), 20 min (c, d), 30 min (e, f) and 120 min (g, h).

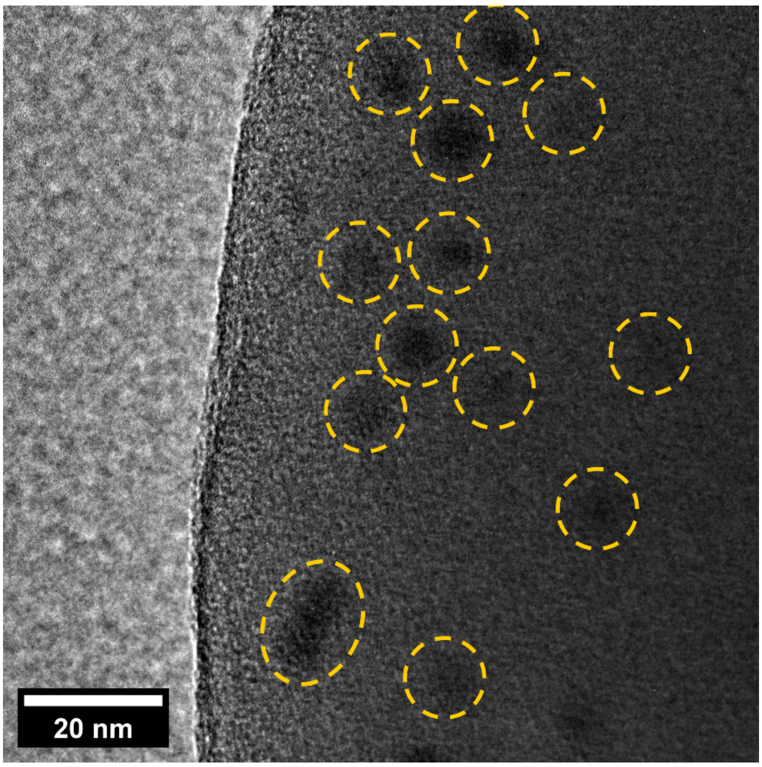

Fig. S2. TEM image of CoO_x/CS composites.

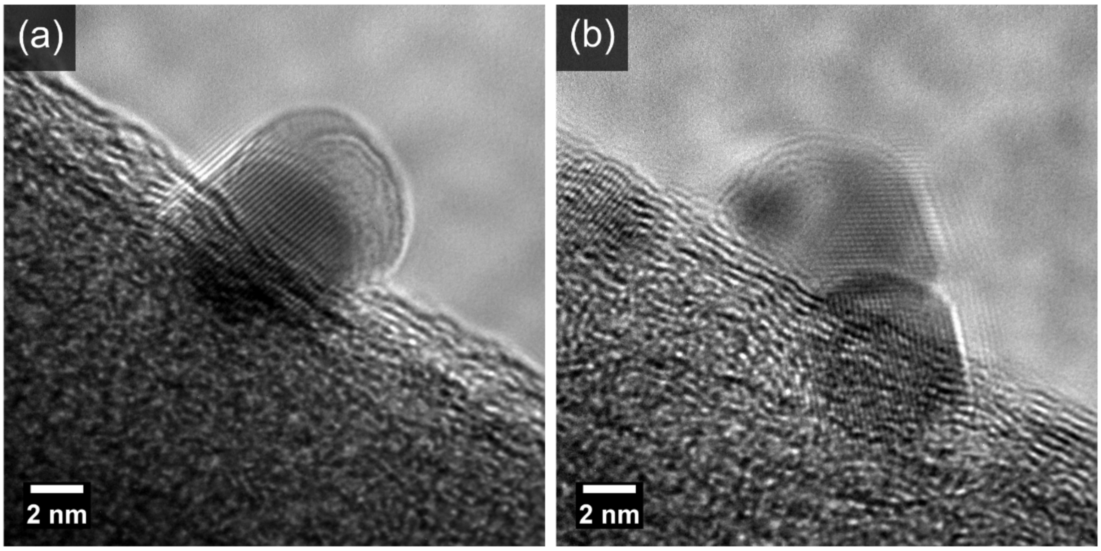

Fig. S3. HRTEM images of CoO_x nanoparticles.

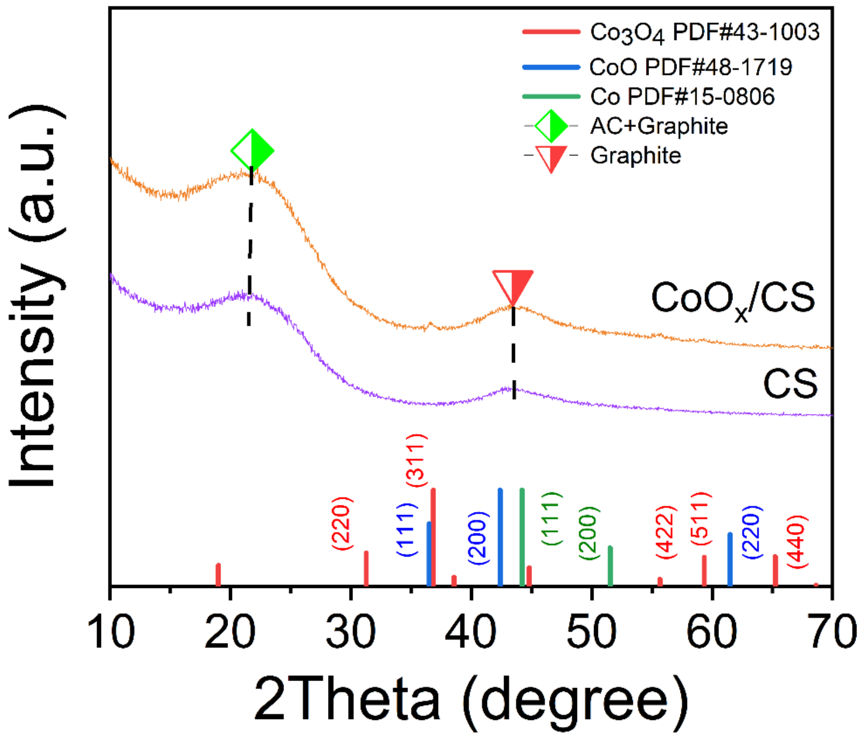

Fig. S4. XRD patterns of CS and CoO_x/CS composites heated at 600 °C for 20 min.

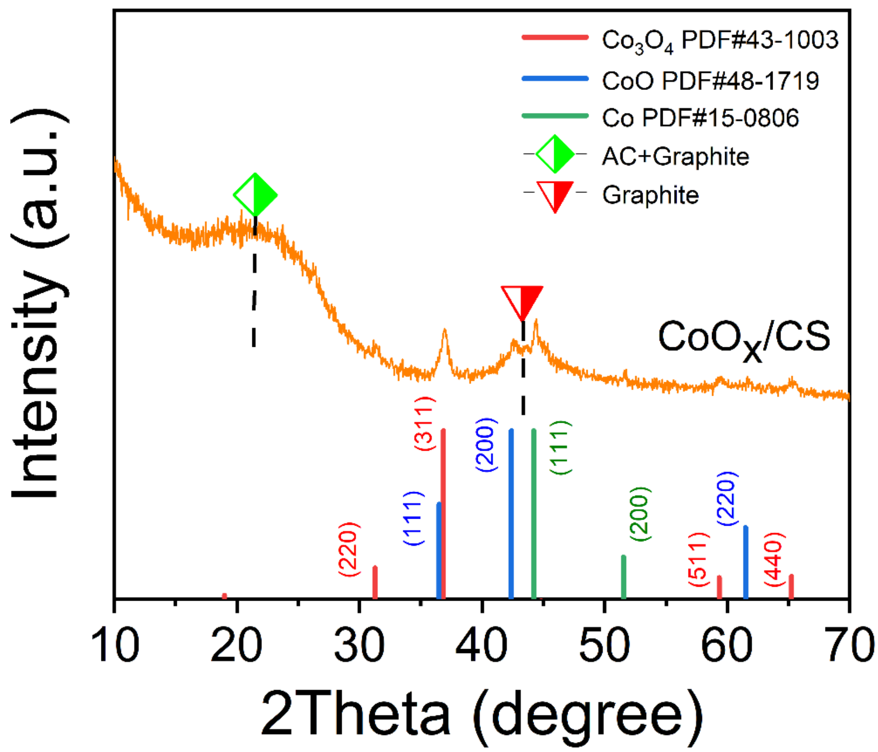

Fig. S5. XRD pattern of CoO_x/CS composites heated at 600 ^{o}C for 2 h.

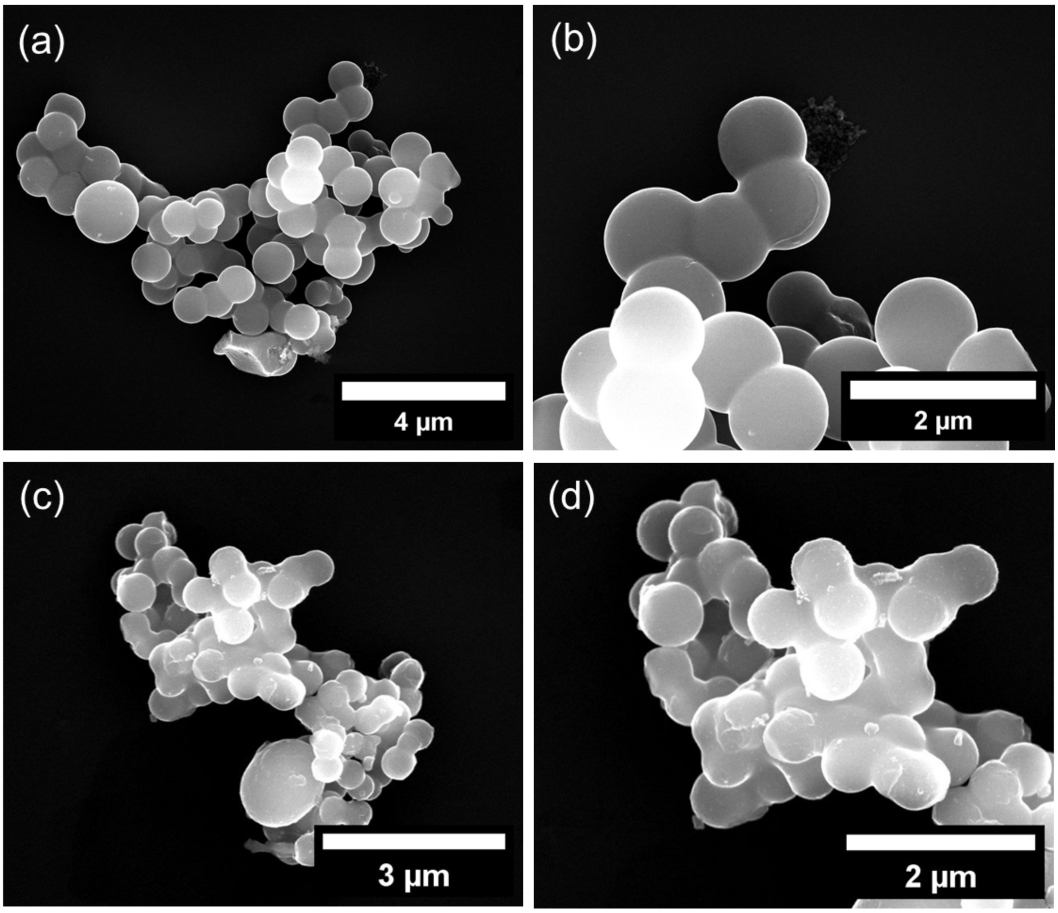

Fig. S6. SEM images of CS (a, b) and CoO_x/CS composites (c, d).

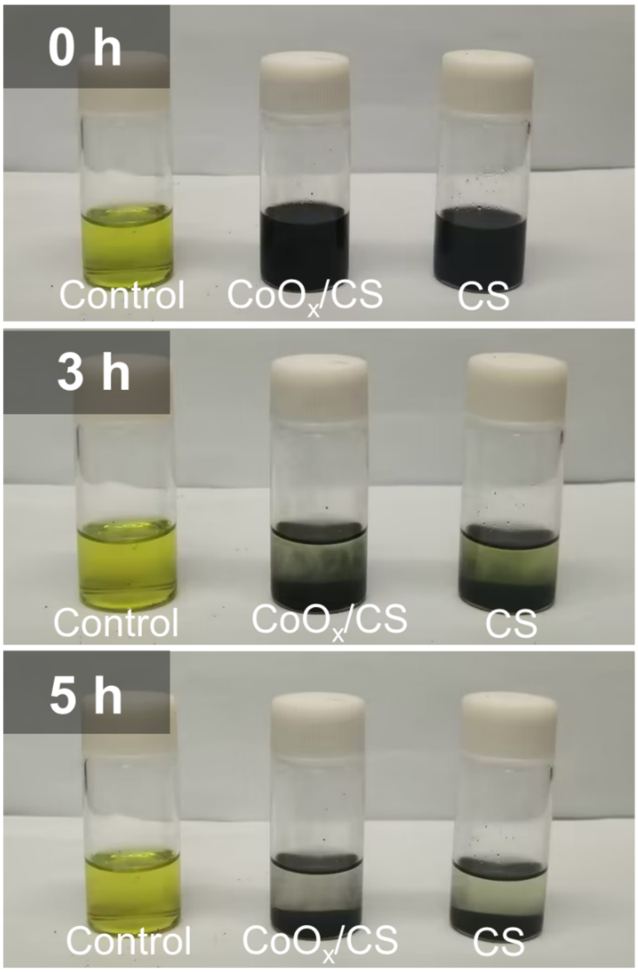

Fig. S7. Visual adsorption results of CoO_x/CS and CS powders in Li_2S_6 solution.

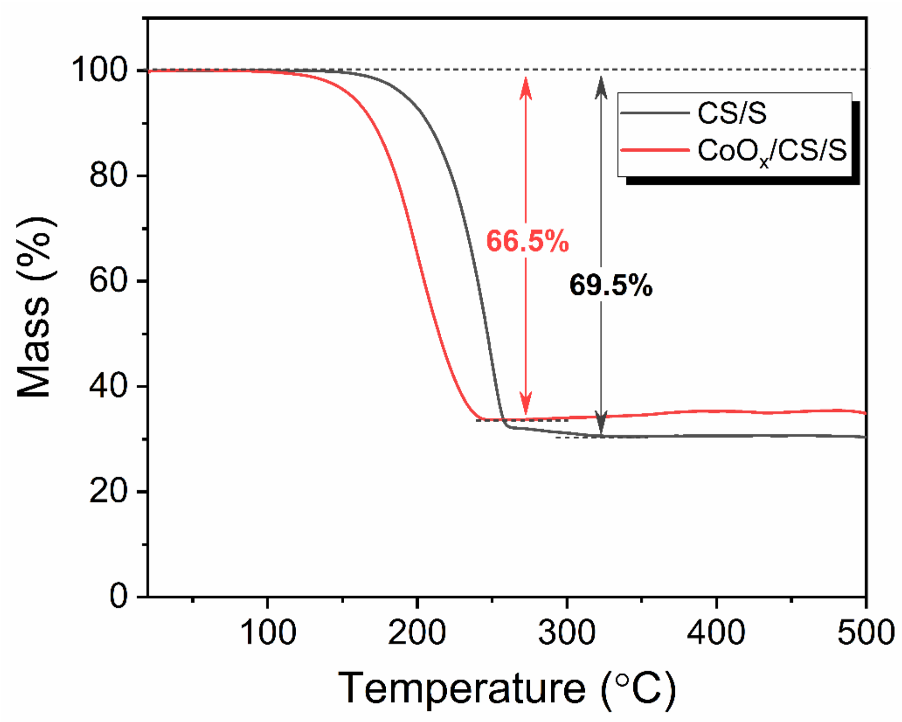

Fig. S8. TG analysis curves of CS/S and CoO_x/CS/S electrode materials under N_2 flow.

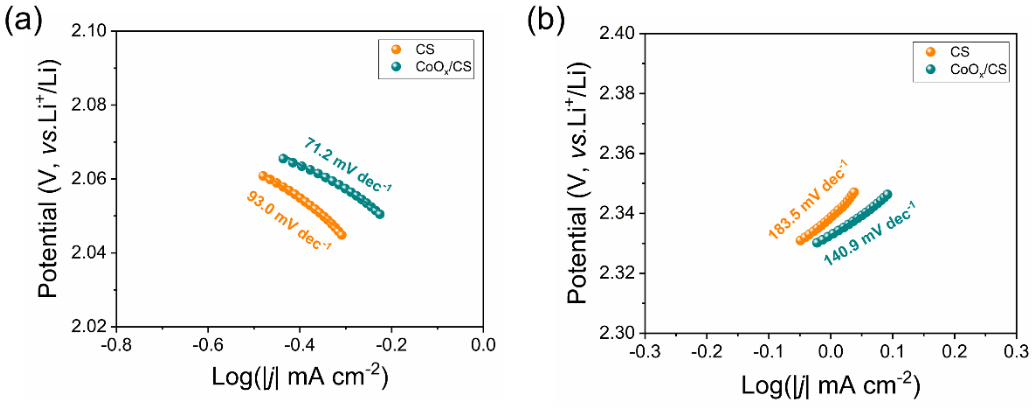

Fig. S9. Tafel plots calculated from reduction peak at 2.0 V (a) and oxidation peak at 2.4 V (b) in Fig. 5a.

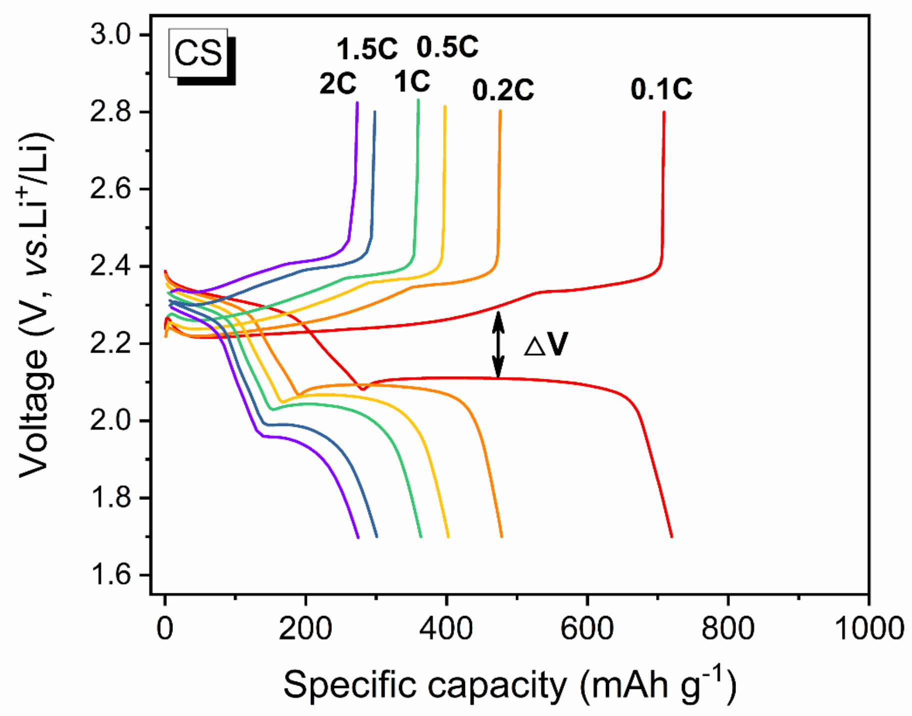

Fig. S10. Galvanostatic charge-discharge profile of CS/S electrode at various current densities.

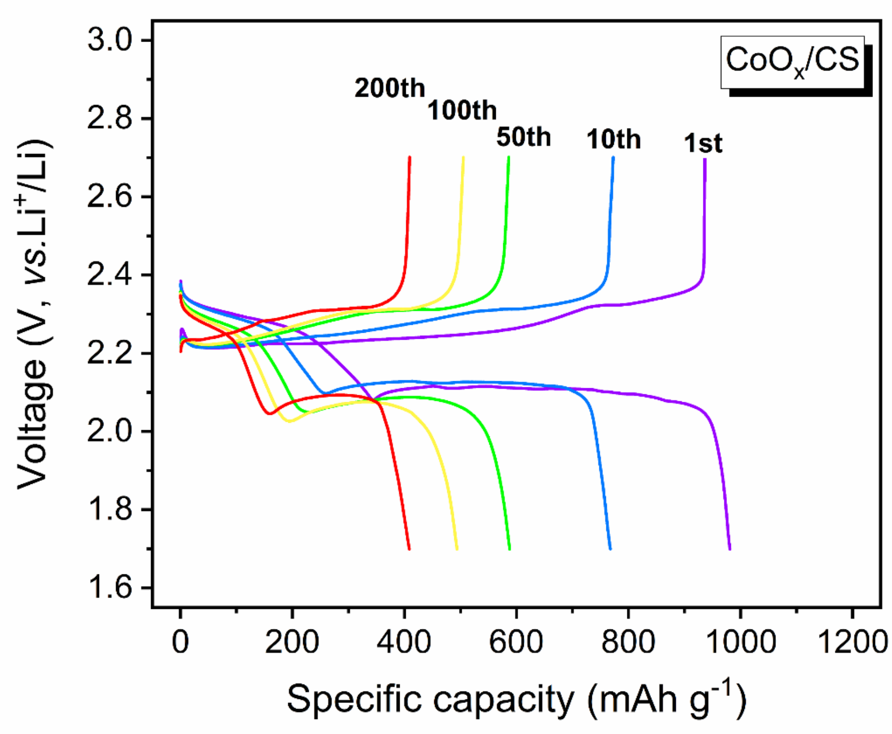

Fig. S11. Galvanostatic discharge/charge profiles of CoO_x/CS full battery cycling at 0.1 C.

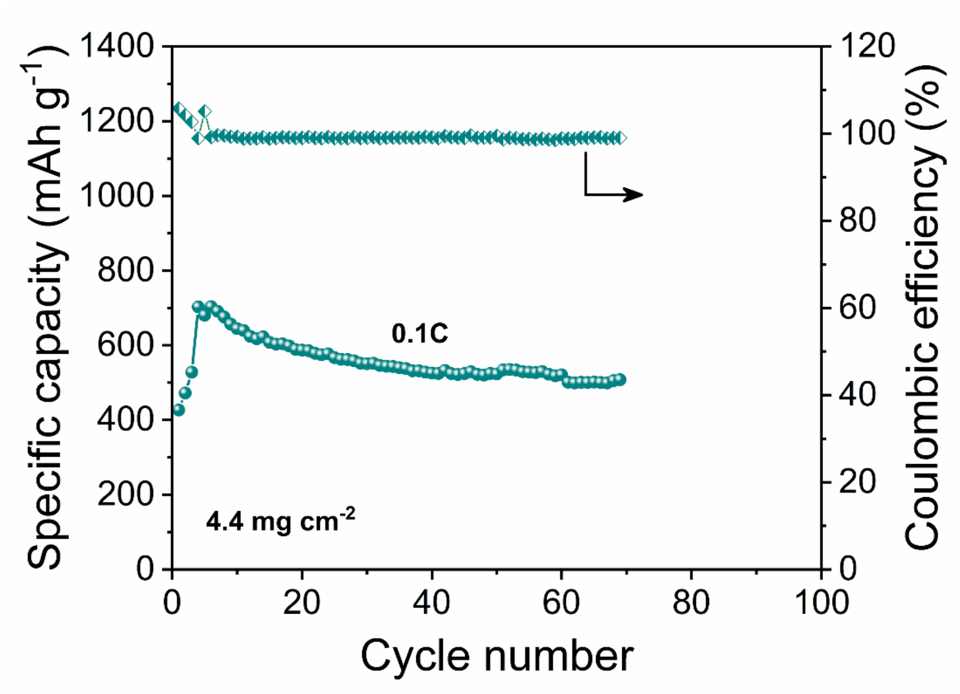

Fig. S12. Cycling performance of CoO_x/CS electrode with high S loading of 4.4 mg cm^{-2}.

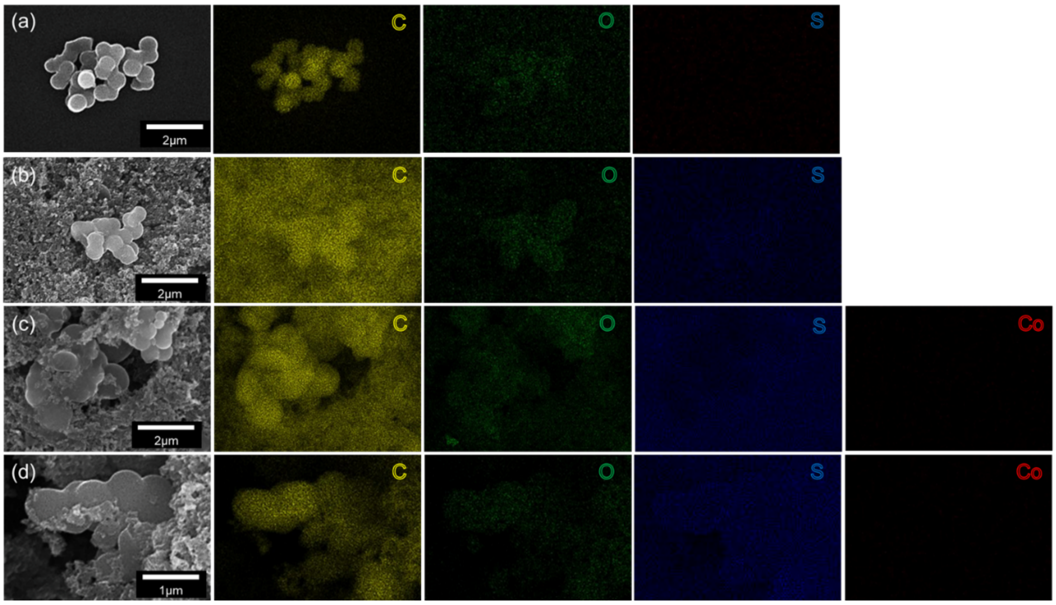

Fig. S13. SEM images and EDX elemental maps of CoO_x/CS composites (a), CS/CS composites (after cycling) (b), CoO_x/CS/S electrode (before cycling) (c), and CoO_x/CS/S electrode (after cycling) (d).

The physical confinement of LiPSs from CS matrix, which has been verified by our recent work[1], could play an important role in inhibiting shuttle effect.

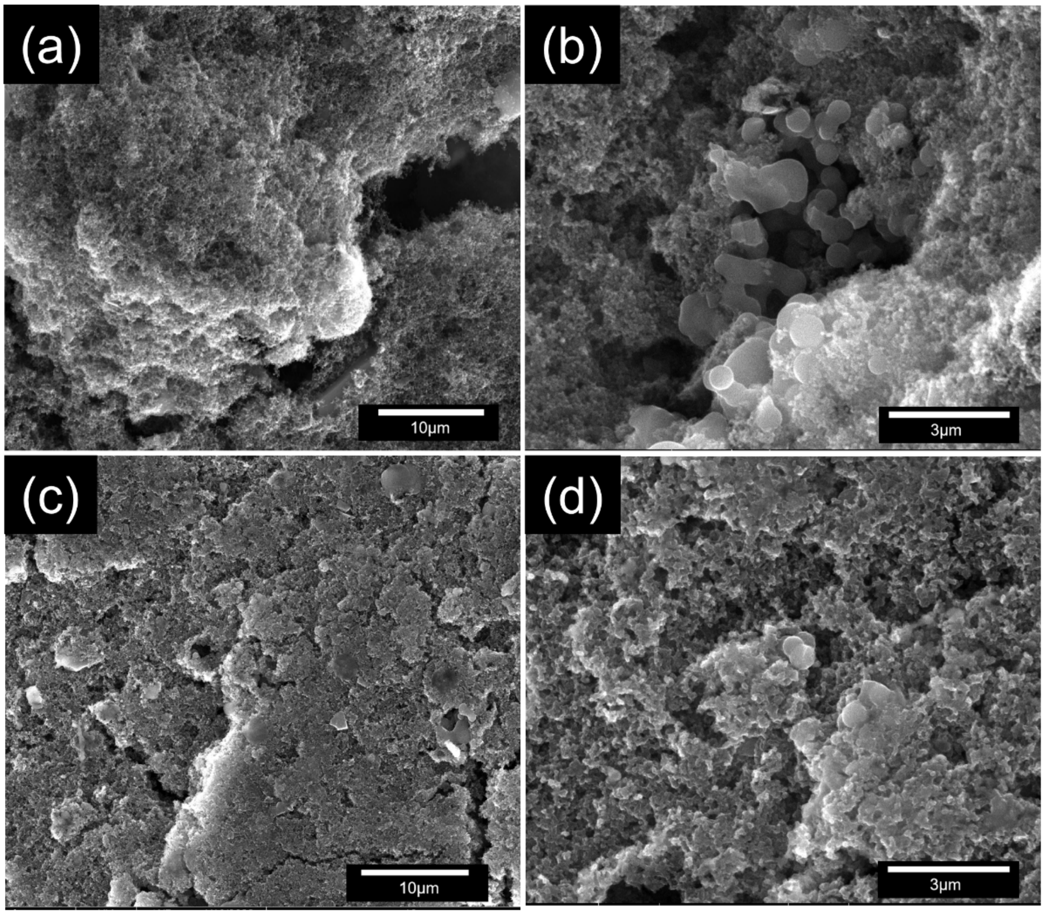

Fig. S14. SEM images of CoO_x/CS/S composites before cycling (a, b) and after cycling (c, d).

Table S1. The surface area, pore volume and pore size of CS and CoO_x/CS composites heated at 600 ^oC for 20 min.

Samples	S_{BET}(m^2 g^{-1})	Pore Volume (cm^{-3} g^{-1})	Pore Size (nm)
CS	325.1	0.137	1.7
CoO_x/CS composites	473.5	0.199	1.7

Table S2. The relative contents of various bond configurations in C 1s high resolution XPS spectra.

Samples	Relative content (%)			
	C-C	C-O	C=O	O-C=O
CS	82.4	9	4.6	4
CoO_x/CS	83.3	9.4	4.2	3.1

Table S3. The relative contents of various bond configurations in O 1s high resolution XPS spectra.

Samples	Relative content (%)			
	Co-O	C-O	C=O	O-C=O
CS	0	27.1	30.8	42.1
CoO_x/CS	15.7	18.7	24.8	40.8

Table S4. The relative contents of various bond configurations in C 1s high resolution XPS spectra of CoO_x/CS electrode before and after cycling.

Samples	Relative content (%)			
	C-C	C-O/C-S	C=O	O-C=O
CoO_x/CS/S before cycling	66.1	16.2	4.0	13.7
CoO_x/CS/S after cycling	69.3	12.6	5.4	12.7

Table S5. The relative contents of various bond configurations in O 1s high resolution XPS spectra of CoO_x/CS electrode before and after cycling.

Samples	Relative content (%)				
	Co-O	C-O	C=O	O-C=O	S-O
CoO_x/CS/S before cycling	1.4	0.4	64.5	16.2	17.5
CoO_x/CS/S after cycling	5.5	0.1	41.5	11.3	41.6

Table S6. The relative contents of various bond configurations in S 2p high resolution XPS spectra of CoO_x/CS/S electrode before and after cycling.

Samples	Relative content (%)				
	Sulfide	S-S	Sulfite	Thiosulfate	Sulfate
CoO_x/CS/S before cycling	0.9	11.7	18.6	34.7	34.1
CoO_x/CS/S after cycling	8.1	5.5	31.0	35.2	20.2

Table S7. The relative contents of various bond configurations in Co 2p high resolution XPS spectra of CoO_x/CS composites and CoO_x/CS/S electrode before and after cycling.

Samples	Relative content (%)			
	Co	Co-O	Co-S	Sat.
CoO_x/CS composites	44.4	27.8	0	27.8
CoO_x/CS/S before cycling	25.6	10.0	22.8	41.6
CoO_x/CS/S after cycling	15.4	17.2	32.6	34.8

References

[1] Y.J. Qi, N. Chai, Q.H. Gu, J.N. Chen, M. Lu, X. Zhang, B.S. Zhang, Chem. Eng. J. 435 (2022) 135112.